PHYSICAL REVIEW A **78**, 011602(R) (2008)

Atom-atom correlations and relative number squeezing in dissociation of spatially inhomogeneous molecular condensates

Magnus Ögren and K. V. Kheruntsyan

ARC Centre of Excellence for Quantum-Atom Optics, School of Physical Sciences, University of Queensland, Brisbane, Queensland 4072, Australia

(Received 26 February 2008; published 16 July 2008)

We study atom-atom correlations and relative number squeezing in the dissociation of a Bose-Einstein condensate (BEC) of molecular dimers made of either bosonic or fermionic atom pairs. Our treatment addresses the role of the spatial inhomogeneity of the molecular BEC on the strength of correlations in the short time limit. We obtain explicit analytic results for the density-density correlation functions in momentum space, and show that the correlation widths and the degree of relative number squeezing are determined merely by the shape of the molecular condensate.

DOI: 10.1103/PhysRevA.78.011602 PACS number(s): 03.75.Nt, 03.65.−w, 05.30.−d, 33.80.Gj

Dissociation of a Bose-Einstein condensate (BEC) of molecular dimers [1] into pair-correlated atoms represents the matter-wave analog of two-photon parametric down-conversion. The latter process has been of crucial importance to the development of quantum optics. Owing to this analogy, molecular dissociation currently represents one of the "workhorses" of the new field of quantum-atom optics [2–10] and offers promising opportunities for the generation of strongly correlated atomic ensembles and fundamental tests of quantum mechanics with macroscopic numbers of massive particles. Examples include the demonstration of the Einstein-Podolski-Rosen paradox and violation of a classical Cauchy-Schwartz inequality [5,8,11]. A closely related process is atomic four-wave mixing in a collision of two BECs [12,13], which produces a spherical halo of spontaneously scattered atoms [14–20] with correlations very similar to those in dissociation.

A recently emerged discussion topic—following the experiments of Ref. [13] on BEC collisions—is the understanding of the width and the strength of the observed correlations, as well as the prospects of detecting relative number squeezing in the halo of the *s*-wave scattered atoms [17,19,20]. The same questions are relevant to atom-atom correlations in molecular dissociation and have not been fully addressed so far.

In this paper, we study atom-atom correlations and relative number squeezing in the dissociation of a molecular BEC in the short time limit. Our analysis applies to molecules that may consist of pairs of either bosonic or fermionic atoms, and takes into account the spatial inhomogeneity of the molecular BEC. It has been argued before and shown in the bosonic case [7,8] that the treatment of spatial inhomogeneity is crucial for obtaining quantitatively correct results for atom-atom correlations. In the fermionic case, the treatments of dissociation have been so far restricted only to uniform systems [6,9,21,22]. In all cases, however, the techniques are numerical and do not give the transparency of analytic understanding, in contrast to the results obtained here.

The effective quantum field theory Hamiltonian describing our system in the undepleted molecular field approximation is given, in a rotating frame, by [23]

$$\hat{H}=\int dx\Bigg\{\sum_{i=1,2}\left(\frac{\hbar^2}{2m}|\partial_x\hat{\Psi}_i|^2+\hbar\Delta\hat{\Psi}_i^\dagger\hat{\Psi}_i\right)-i\hbar g(x)(\hat{\Psi}_1\hat{\Psi}_2-\hat{\Psi}_2^\dagger\hat{\Psi}_1^\dagger)\Bigg\}. \quad (1)$$

The operators $\hat{\Psi}_{1,2}(x,t)$ describe the atoms in two different spin states, which can be either bosonic or fermionic, and we assume that they have the same mass. The effective coupling $g(x)$ is defined as $g(x)=\chi\sqrt{\rho_0(x)}$, where χ is the atom-molecule coupling (see [22] for details) and $\rho_0(x)$ is the initial density of the molecular BEC in a harmonic trap. For computational simplicity, we start by treating a one-dimensional (1D) system; the analytic results will later be generalized to three dimensions (3D).

The key difference between the present and previous (uniform) treatments of dissociation in the undepleted molecular approximation [4,6] is that we retain the spatial dependency of the molecular BEC: the effective coupling $g(x)$ absorbs the molecular field, which is treated classically via the coherent mean-field amplitude $\Psi_0(x)=\sqrt{\rho_0(x)}$. The undepleted molecular approximation is valid only for short dissociation times, during which the converted fraction of molecules does not exceed ~10% [7,22]. Accordingly, the coupling $g(x)$ can be kept constant in time, although the evolution of the atomic field is taking place in free space. In this regime, the dissociation typically creates low-density atomic clouds for which the *s*-wave scattering interactions are a negligible effect too [7].

The detuning Δ in Eq. (1) corresponds to the energy mismatch $2\hbar\Delta$ between the free two-atom state in the dissociation threshold and the bound molecular state. Molecules that are unstable against spontaneous dissociation correspond to $\Delta<0$, with $2\hbar|\Delta|$ being the total dissociation energy that is converted into kinetic energy of atom pairs primarily populating the resonant momenta around $\pm k_0$, with $k_0=\sqrt{2m|\Delta|}/\hbar$.

Writing down the Heisenberg equations of motion for the field operators and converting to Fourier space $\hat{\Psi}_j(x,t)=\int dk\hat{a}_j(k,t)\exp(ikx)/\sqrt{2\pi}$, we arrive at the following coupled equations for the operators $\hat{a}_j(k,t)$:

$$\frac{d\hat{a}_1(k,t)}{dt} = -i\Delta_k \hat{a}_1(k,t) \pm \int \frac{dq}{\sqrt{2\pi}} \tilde{g}(q+k)\hat{a}_2^\dagger(q,t),$$

$$\frac{d\hat{a}_2^\dagger(k,t)}{dt} = i\Delta_k \hat{a}_2^\dagger(k,t) + \int \frac{dq}{\sqrt{2\pi}} \tilde{g}(q-k)\hat{a}_1(-q,t). \quad (2)$$

Here and hereafter, the + (−) [in general, upper (lower)] sign stands for bosonic (fermionic) statistics of the atoms, $\tilde{g}(k)=\int dx e^{-ikx} g(x)/\sqrt{2\pi}$ is the Fourier transform of the effective coupling $g(x)$, and $\Delta_k \equiv \hbar k^2/(2m_1)+\Delta$.

Equations (2) can be solved numerically using standard methods of linear operator algebra. One can show that, for vacuum initial conditions, the only nonzero second-order moments are the normal and anomalous atomic densities, $n_j(k,k',t) \equiv \langle \hat{a}_j^\dagger(k,t)\hat{a}_j(k',t)\rangle$ and $m_{12}(k,k',t) \equiv \langle \hat{a}_1(k,t)\hat{a}_2(k',t)\rangle$. From Eqs. (2) we can see that the finite width of $\tilde{g}(k)$—due to the inhomogeneity of the source—implies that $\hat{a}_1(k)$ couples not only to the partner spin component at exactly opposite momentum $\hat{a}_2^\dagger(-k)$ (as is the case in the homogeneous system), but also to a range of momenta around $-k$, within $-k \pm \delta k$. The spread in δk determines the width of atom-atom correlations and is ultimately related to the width of the molecular BEC.

We now turn to the quantitative analysis of atom-atom correlations expected to be present between the different spin-state atoms with equal but opposite momenta due to momentum conservation, and between the same spin-state atoms in the collinear direction due to quantum statistical effects. We quantify these correlations via Glauber's second-order correlation function,

$$g_{ij}^{(2)}(k,k',t) = \frac{\langle \hat{a}_i^\dagger(k,t)\hat{a}_j^\dagger(k',t)\hat{a}_j(k',t)\hat{a}_i(k,t)\rangle}{n_i(k,t)n_j(k',t)}. \quad (3)$$

The normalization with respect to the product of densities $n_i(k,t)$ and $n_j(k',t)$ [with $n_j(k,t) \equiv n_j(k,k,t)$] ensures that $g_{ij}^{(2)}(k,k',t)=1$ for uncorrelated states. Due to obvious symmetry considerations, $g_{12}^{(2)}(k,k',t)=g_{21}^{(2)}(k,k',t)$ and $g_{11}^{(2)}(k,k',t)=g_{22}^{(2)}(k,k',t)$.

Since the effective Hamiltonian corresponding to Eqs. (2) is quadratic in the field operators, we can apply Wick's theorem to factorize the fourth-order moment in Eq. (3). Noting that $\langle \hat{a}_1^\dagger(k,t)\hat{a}_2(k',t)\rangle = \langle \hat{a}_j(k,t)\hat{a}_j(k',t)\rangle = 0$ in the present model, we obtain

$$g_{12}^{(2)}(k,k',t) = 1 + |m_{12}(k,k',t)|^2/[n_1(k,t)n_2(k',t)], \quad (4)$$

$$g_{jj}^{(2)}(k,k',t) = 1 \pm |n_j(k,k',t)|^2/[n_j(k,t)n_j(k',t)]. \quad (5)$$

Before presenting the results based on numerical solutions of Eqs. (2), we now develop simple analytic approaches that give approximate predictions for these observables, valid for short times. More specifically, we treat the short time dynamics of dissociation via the Taylor expansion in time, up to terms of order t^2 [26],

$$\hat{a}_j(k,t) = \hat{a}_j(k,0) + \left.\frac{\partial \hat{a}_j(k,t)}{\partial t}\right|_{t=0} t + \left.\frac{\partial^2 \hat{a}_j(k,t)}{\partial t^2}\right|_{t=0} \frac{t^2}{2} + \cdots$$

valid for $t \ll t_0$, where $t_0 = 1/\chi\sqrt{\rho_0(0)}$ is the time scale. Using the rhs of Eqs. (2), this gives, up to the lowest-order terms, $n_j(k,k',t) \simeq t^2 \int dq \tilde{g}^*(q+k)\tilde{g}(q+k')/2\pi$ and $|m_{12}(k,k',t)| \simeq t|\tilde{g}(k+k')|/\sqrt{2\pi}$, or equivalently

$$n_j(k,k',t) \simeq t^2 \int dx e^{-i(k-k')x}[g(x)]^2/2\pi, \quad (6)$$

$$|m_{12}(k,k',t)| \simeq t\left|\int dx e^{-i(k+k')x} g(x)/2\pi\right|. \quad (7)$$

These results show that the width of the collinear (CL) correlation between the same-spin atoms with nearly the same momenta, Eq. (5), will be determined by the square of the Fourier transform of the square of the effective coupling $g(x)$. On the other hand, the width of the back-to-back (BB) correlation, Eq. (4), between the different spin-state atoms with nearly opposite momenta will be determined by the square of the Fourier transform of $g(x)$. Therefore, the CL correlation is generally broader than the BB correlation. These conclusions are true for any shape of the source and apply to both bosonic and fermionic statistics in the short time limit.

Thomas-Fermi (TF) parabolic density profile. We now give explicit analytic results for the case of a TF inverted parabola for the molecular BEC density, $\rho_0(x)=\rho_0(1-x^2/R_{\rm TF}^2)$ $(|x| \leqslant R_{\rm TF})$, in which case $g(x) = \chi\sqrt{\rho_0}(1-x^2/R_{\rm TF}^2)^{1/2}$. Using the integral representation of Bessel functions $J_\nu(z)$ [27], Eqs. (6) and (7) yield

$$n_j(k,k',t) \simeq \frac{2t^2\chi^2\rho_0 R_{\rm TF}}{\sqrt{2\pi}} \frac{J_{3/2}((k-k')R_{\rm TF})}{[(k-k')R_{\rm TF}]^{3/2}}, \quad (8)$$

$$|m_{12}(k,k',t)| \simeq \frac{t\chi\sqrt{\rho_0}R_{\rm TF}}{2} \frac{J_1((k+k')R_{\rm TF})}{(k+k')R_{\rm TF}}. \quad (9)$$

Since $J_\nu(z) \simeq (z/2)^\nu/\Gamma(\nu+1)$ for $z \ll 1$, the atomic momentum distribution $n_j(k,t)$ and the diagonal anomalous density $m_{12}(k,-k,t)$ are $n_j(k,t) \simeq 2t^2\chi^2\rho_0 R_{\rm TF}/3\pi$ and $|m_{12}(k,-k,t)| \simeq t\chi\sqrt{\rho_0}R_{\rm TF}/4$. Despite the fact that the atomic momentum distribution in the lowest order in t is uniform, the momentum cutoff $k_{\rm max}$ [23]—which must be assumed when using a δ-function interaction in Eq. (1)—prevents the total atom number from diverging.

Substituting Eqs. (8) and (9) into Eqs. (4) and (5), we obtain the following explicit results for the atom-atom correlations, valid for $t \ll t_0$:

$$g_{12}^{(2)}(k,k',t) \simeq 1 + \frac{9\pi^2}{16t^2\chi^2\rho_0} \frac{[J_1((k+k')R_{\rm TF})]^2}{[(k+k')R_{\rm TF}]^2}, \quad (10)$$

$$g_{jj}^{(2)}(k,k',t) \simeq 1 \pm \frac{9\pi}{2} \frac{[J_{3/2}((k-k')R_{\rm TF})]^2}{[(k-k')R_{\rm TF}]^3}. \quad (11)$$

The pair correlations $g_{ij}^{(2)}(k,k_0,t=0.5t_0)$, where the momentum of one of the atomic components is fixed to k_0,

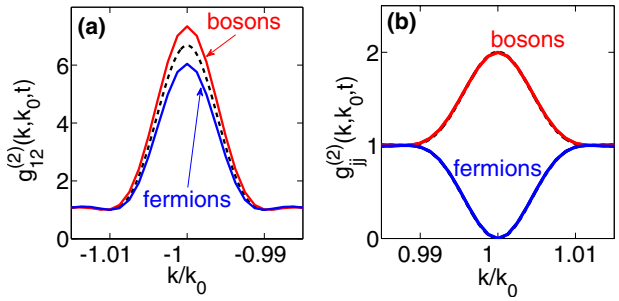

FIG. 1. (Color online) Back-to-back (a) and collinear (b) correlation $g_{ij}^{(2)}(k,k_0,t)$ as a function of k at $t/t_0=0.5$. The dimensionless detuning is $\delta=\Delta t_0=-9$, where $t_0=1/\chi\sqrt{\rho_0(0)}\simeq 5$ ms is the time scale; the Thomas-Fermi radius of the molecular BEC is $R_{\mathrm{TF}}=250$ μm; for other parameters, see Ref. [24].

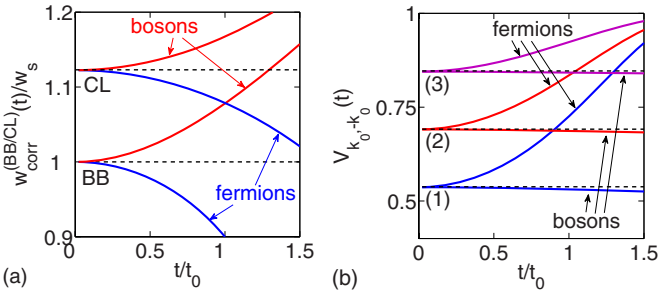

FIG. 2. (Color online) (a) Width of the BB and CL correlations relative to the momentum width of the molecular BEC, $w_s \simeq 1.62/R_{\mathrm{TF}}$, as a function of time, for the physical parameters of Fig. 1. (b) Relative number variance $V_{k_0,-k_0}(t)$ as a function of time, for $R_{\mathrm{TF}}^{(1)}=250$ μm (1), $R_{\mathrm{TF}}^{(2)}=167$ μm (2), and $R_{\mathrm{TF}}^{(3)}=83$ μm (3). The counting length is $\Delta k=\pi/2R_{\mathrm{TF}}^{(1)}$ in all cases.

while the partner momentum k is varied, is plotted in Figs. 1(a) and 1(b). The dashed lines are the analytic results of Eqs. (10) and (11), whereas the solid lines are the numerical results from Eqs. (2). In Fig. 1(b), the dashed lines are almost indistinguishable from the respective solid lines, even though the ratio $t/t_0=0.5$ is not very small. For earlier times, the agreement between the analytic and numerical results is even better.

In the case of different spin states, $g_{12}^{(2)}(k,k_0,t)$, with either bosonic or fermionic atoms, we see a strong BB correlation signal between atom pairs with equal but opposite momenta, centered at $k=-k_0$. The same-spin CL correlation function $g_{jj}^{(2)}(k,k_0,t)$, on the other hand, shows the Hanbury Brown and Twiss bunching peak for bosons and an antibunching dip for fermions due to Pauli blocking [25], both centered at $k=k_0$.

In Fig. 2(a), we plot the widths of the BB and CL correlations as a function of time. For simplicity, we define them as the half-width at half-maximum. The widths in the bosonic and fermionic cases (with the solid lines corresponding to the numerical results) have universal asymptotics in the limit $t\to 0$, when the quantum statistical effects are irrelevant due to low mode occupancies. The asymptotic values (dashed lines) are found from Eqs. (10) and (11): $w_{\mathrm{corr}}^{(\mathrm{BB})}=w_s$ and $w_{\mathrm{corr}}^{(\mathrm{CL})}\simeq 1.12w_s$, where $w_s\simeq 1.62/R_{\mathrm{TF}}$ is the width of the momentum distribution $\tilde{\rho}_0(k)=|\tilde{g}(k)|^2/\chi^2=|\sqrt{\rho_0}\pi/2J_1(kR_{\mathrm{TF}})/k|^2$ of the actual source—the molecular BEC.

As an alternative measure of the strength of atom-atom correlations [7], we also calculate the normalized variance of number-difference fluctuations for atoms in different spin states and with equal but opposite momenta $\pm k_0$,

$$V_{k_0,-k_0}(t)=\langle[\Delta(\hat{N}_{1,k_0}-\hat{N}_{2,-k_0})]^2\rangle/N_S, \tag{12}$$

where N_S is the shot-noise level that originates from uncorrelated states. The number operators are defined by $\hat{N}_{j,\pm k_0}(t)=\int_K dk\hat{n}_j(k,t)$ [with $\hat{n}_j(k,t)=\hat{a}_j^\dagger(k,t)\hat{a}_j(k,t)$], where K is the counting length around $\pm k_0$. On a computational lattice, the simplest choice that does not require explicit binning of the signal is $K=\Delta k$, where Δk is the lattice spacing, and therefore $\hat{N}_{j,\pm k_0}(t)=\hat{n}_j(\pm k_0,t)\Delta k$. We emphasize that N_S is different for bosons and fermions. For the bosonic case, N_S is given by the sum of variances of the individual mode occupancies with Poissonian statistics (as in the coherent state), implying that $N_S=\langle\hat{N}_{1,k_0}\rangle+\langle\hat{N}_{2,-k_0}\rangle$. For the fermionic case, the sum of individual variances gives $N_S=\langle\hat{N}_{1,k_0}\rangle(1-\langle\hat{N}_{1,k_0}\rangle)+\langle\hat{N}_{2,-k_0}\rangle(1-\langle\hat{N}_{2,-k_0}\rangle)$ [6]. The variance (12) can be rewritten as

$$V_{k_0,-k_0}(t)=1-\frac{\Delta k n_1(k_0,t)}{1-s\Delta k n_1(k_0,t)}\times[g_{12}^{(2)}(k_0,-k_0,t)-g_{11}^{(2)}(k_0,k_0,t)], \tag{13}$$

where $s=0(1)$ for bosons (fermions), and we have taken into account that $\langle\hat{N}_{1,k_0}\rangle=\langle\hat{N}_{2,-k_0}\rangle$ and $g_{11}^{(2)}(k_0,k_0,t)=g_{22}^{(2)}(-k_0,-k_0,t)$. Variance $V_{k_0,-k_0}(t)<1$ implies squeezing of fluctuations below the shot-noise level and corresponds to a violation of the classical Cauchy-Schwartz inequality with $g_{12}^{(2)}(k_0,-k_0,t)>g_{11}^{(2)}(k_0,k_0,t)$ [8].

The short time asymptotics for the variance can be found using Eqs. (10) and (11), yielding

$$V_{k_0,-k_0}(t\ll t_0)=1-3\pi\Delta kR_{\mathrm{TF}}/32. \tag{14}$$

The small geometric prefactor in the second term, together with the resolution requirement $\Delta k\lesssim 1/R_{\mathrm{TF}}$, ensures that $V_{k_0,-k_0}>0$. We see that the squeezing is stronger for larger condensates and counting lengths.

In Fig. 2(b) we plot the variance $V_{k_0,-k_0}(t)$ for three different sizes of the molecular condensate. The solid lines are the numerical results from Eqs. (2), whereas the horizontal dashed lines are the short time asymptotic results of Eq. (14) matching precisely the numerical results in the limit $t\to 0$. As we can see, the squeezing of the relative number fluctuations (from the numerical curves) does not change significantly with time for bosons, while for fermions its dynamics is affected by a stronger dependence of the fermionic shot noise on the mode occupancy. The squeezing is stronger for larger condensates, but is still far from perfect squeezing, $V_{k_0,-k_0}(t)=0$, which follows from the idealized uniform models [6,7].

Gaussian density profile. For comparison, we also give the analytic results for a Gaussian density profile $\rho_0(x)=\rho_0\exp(-x^2/2\sigma_x^2)$ of the molecular BEC, giving the momentum distribution of $\tilde{\rho}_0(k)\propto\exp(-k^2/2\sigma_k^2)$, where σ_x and $\sigma_k=1/2\sigma_x$ are the rms widths. In this case, the atom-atom correlations are

$$g_{12}^{(2)}(k,k',t\ll t_0)\simeq 1+2e^{-(k+k')^2/2\sigma_k^2}/(t^2\chi^2\rho_0), \quad (15)$$

$$g_{jj}^{(2)}(k,k',t\ll t_0)\simeq 1\pm e^{-(k-k')^2/4\sigma_k^2}. \quad (16)$$

The respective rms widths are given by $\sigma_{\mathrm{corr}}^{(\mathrm{BB})}=\sigma_k$ and $\sigma_{\mathrm{corr}}^{(\mathrm{CL})}=\sqrt{2}\sigma_k$, resulting in the ratio $\sigma_{\mathrm{corr}}^{(\mathrm{CL})}/\sigma_{\mathrm{corr}}^{(\mathrm{BB})}=\sqrt{2}$. The relative number squeezing is $V_{k_0,-k_0}(t\ll t_0)=1-\sqrt{2/\pi}\Delta k\sigma_x$, with $\Delta k\lesssim 1/2\sigma_x$ ensuring $V_{k_0,-k_0}>0$.

Results in 3D. For a nonisotropic TF parabolic density profile of the molecular BEC, performing the integrals in 3D versions of Eqs. (6) and (7) is more cumbersome and we only give the final results for correlations corresponding to the displacement between the pairs of momenta along one of the Cartesian coordinates $\alpha=x,y,z$. The BB and CL correlation widths obtained here are $w_{\mathrm{corr},\alpha}^{(\mathrm{BB})}=w_{s,\alpha}$ and $w_{\mathrm{corr},\alpha}^{(\mathrm{CL})}\simeq 1.08w_{s,\alpha}$, where $w_{s,\alpha}\simeq 1.99/R_{\mathrm{TF},\alpha}$. The relative number variance is $V_{k_0,-k_0}(t\ll t_0)\simeq 1-15(\overline{\Delta k}R_{\mathrm{TF}})^3/2^{10}$, where $\overline{\Delta k}=(\Delta k_x\Delta k_y\Delta k_z)^{1/3}$ and $\overline{R_{\mathrm{TF}}}=(R_{\mathrm{TF},x}R_{\mathrm{TF},y}R_{\mathrm{TF},z})^{1/3}$ are the geometric means. The much smaller (than in 1D) geometric prefactor in the second term, together with $\Delta k_\alpha\lesssim 1/R_{\mathrm{TF},\alpha}$, explains why the "raw" (unbinned) squeezing is much weaker in 3D [7,8] than in 1D. Therefore, the prescription of Ref. [8] to perform binning for obtaining stronger squeezing is more crucial in 3D.

For a Gaussian density profile, the generalization to 3D is straightforward. In particular, the BB and CL correlation widths for a displacement along x, y, or z are as in 1D, while the relative number variance is $V_{k_0,-k_0}(t\ll t_0)=1-[\sqrt{2/\pi}\,\overline{\Delta k}\bar{\sigma}]^3$, where $\bar{\sigma}=(\sigma_x\sigma_y\sigma_z)^{1/3}$.

In summary, we have studied the dissociation of a BEC of molecular dimers into correlated fermionic and bosonic atom pairs. We have obtained explicit analytic results for the width and strength of the atom-atom correlations and for the relative number squeezing in the short time limit, using realistic density profiles of the molecular BEC. The results show how the squeezing improves with the larger size of the molecular condensate, and how it can degrade in strongly inhomogeneous systems. Our approach can be easily generalized to describe similar effects in atomic four-wave mixing via BEC collisions [13,19,20].

The authors acknowledge support from the Australian Research Council and thank J. F. Corney, M. J. Davis, M. K. Olsen, and C. M. Savage for useful discussions.

[1] T. Mukaiyama, J. R. Abo-Shaeer, K. Xu, J. K. Chin, and W. Ketterle, Phys. Rev. Lett. **92**, 180402 (2004); S. Dürr, T. Volz, and G. Rempe, Phys. Rev. A **70**, 031601(R) (2004); M. Greiner, C. A. Regal, J. T. Stewart, and D. S. Jin, Phys. Rev. Lett. **94**, 110401 (2005); S. T. Thompson, E. Hodby, and C. E. Wieman, *ibid.* **94**, 020401 (2005).

[2] U. V. Poulsen and K. Mølmer, Phys. Rev. A **63**, 023604 (2001); K. V. Kheruntsyan and P. D. Drummond, *ibid.* **66**, 031602(R) (2002); K. V. Kheruntsyan, *ibid.* **71**, 053609 (2005).

[3] M. G. Moore and A. Vardi, Phys. Rev. Lett. **88**, 160402 (2002); T. Köhler, E. Tiesinga, and P. S. Julienne, *ibid.* **94**, 020402 (2005).

[4] V. A. Yurovsky and A. Ben-Reuven, Phys. Rev. A **67**, 043611 (2003).

[5] K. V. Kheruntsyan, M. K. Olsen, and P. D. Drummond, Phys. Rev. Lett. **95**, 150405 (2005).

[6] K. V. Kheruntsyan, Phys. Rev. Lett. **96**, 110401 (2006).

[7] C. M. Savage, P. E. Schwenn, and K. V. Kheruntsyan, Phys. Rev. A **74**, 033620 (2006).

[8] C. M. Savage and K. V. Kheruntsyan, Phys. Rev. Lett. **99**, 220404 (2007).

[9] M. W. Jack and H. Pu, Phys. Rev. A **72**, 063625 (2005).

[10] B. Zhao *et al.*, Phys. Rev. A **75**, 042312 (2007); I. Tikhonenkov and A. Vardi, Phys. Rev. Lett. **98**, 080403 (2007).

[11] T. Opatrný and G. Kurizki, Phys. Rev. Lett. **86**, 3180 (2001).

[12] L. Deng *et al.*, Nature (London) **398**, 218 (1999); J. M. Vogels, K. Xu, and W. Ketterle, Phys. Rev. Lett. **89**, 020401 (2002).

[13] A. Perrin *et al.*, Phys. Rev. Lett. **99**, 150405 (2007).

[14] H. Pu and P. Meystre, Phys. Rev. Lett. **85**, 3987 (2000).

[15] L.-M. Duan, A. Sorensen, J. I. Cirac, and P. Zoller, Phys. Rev. Lett. **85**, 3991 (2000).

[16] V. A. Yurovsky, Phys. Rev. A **65**, 033605 (2002).

[17] R. Bach, M. Trippenbach, and K. Rzażewski, Phys. Rev. A **65**, 063605 (2002); P. Ziń, J. Chwedenczuk, A. Veitia, K. Rzazewski, and M. Trippenbach, Phys. Rev. Lett. **94**, 200401 (2005).

[18] A. A. Norrie, R. J. Ballagh, and C. W. Gardiner, Phys. Rev. A **73**, 043617 (2006); P. Deuar and P. D. Drummond, Phys. Rev. Lett. **98**, 120402 (2007).

[19] K. Mølmer *et al.*, Phys. Rev. A **77**, 033601 (2008).

[20] A. Perrin *et al.*, New J. Phys. **10**, 045021 (2008).

[21] J. F. Corney and P. D. Drummond, Phys. Rev. Lett. **93**, 260401 (2004); Phys. Rev. B **73**, 125112 (2006).

[22] M. J. Davis, S. J. Thwaite, M. K. Olsen, and K. V. Kheruntsyan, Phys. Rev. A **77**, 023617 (2008).

[23] K. V. Kheruntsyan and P. D. Drummond, Phys. Rev. A **61**, 063816 (2000); P. D. Drummond and K. V. Kheruntsyan, *ibid.* **70**, 033609 (2004).

[24] In the case of fermionic atoms, we consider a BEC of $^{40}K_2$ dimers with a peak 1D density $\rho_0(0)=4\times10^7\ \mathrm{m}^{-1}$ and $\chi=3.15\times10^{-2}\ \mathrm{m}^{1/2}/\mathrm{s}$ [22]. In the bosonic case, we assume the same parameters as a hypothetic example.

[25] These effects are similar to those observed in BEC collisions [13] and in a degenerate Fermi gas; T. Jeltes *et al.*, Nature (London) **445**, 402 (2007).

[26] One can check that the commutation and anticommutation relations here are $[\hat{a}(\mathbf{k},t),\hat{a}^\dagger(\mathbf{k}',t)]_\mp\approx\delta(\mathbf{k}-\mathbf{k}')$ up to terms of the order of t^2.

[27] *Handbook of Mathematical Functions*, edited by M. Abramowitz and I. A. Stegun (Dover, New York, 1965).